Accurate Modeling of Radial Suspension Force on AC Magnetic Bearings

Weiyu Zhang*
School of Electrical and Information Engineering, Jiangsu University
Zhenjiang, China

Huangqiu Zhu
School of Electrical and Information Engineering, Jiangsu University
Zhenjiang, China

Li Cao
School of Electrical and Information Engineering, Jiangsu University
Zhenjiang, China

Abstract

This paper presents a new modeling method based on Maxwell tensor method for radial suspension forces of AC magnetic bearing. Comparing existing method, the invention explicitly designed for AC magnetic bearing is more accurate. Take the AC hybrid magnetic bearing (AC HMB) for example, this paper presents the mathematically modeling process of radial suspension forces with the proposed method. In a comparison of the model established by equivalent magnetic circuit method and by the proposed method, the high uniformity is revealed in its expression form (the only difference is the coefficient between them). To illustrate the precision of the proposed modeling approach, relevant verification experiment are designed and conducted. Indeed, the experimental results show that the proposed modeling method is more accurate than the traditional method (equivalent magnetic circuit method).

1 Introduction

The researchers all over the world have long been committed to research the direct current (DC) magnetic bearing [1-2]. However, many of the research on the alternating current (AC) magnetic bearing until recent years are developed and have aroused wide concern in the public [1]. Here, The AC magnetic bearing is so called because this magnetic bearing can be controlled by AC motor control method to suspend the rotor, which is different from DC magnetic bearing. In a radial DC magnetic bearing, usually four independent electromagnets are arranged around the rotor. They are operated either by four unipolar power amplifiers or by two bipolar amplifiers. A simplification of magnetic bearing can be achieved by the arrangement of only three electromagnets. If regards as it a DC magnetic bearing, that still needs three independent unipolar power amplifiers for controlling the radial part of magnetic bearing. But if regards it as an AC magnetic bearing, that just requires a three-phase power converter which is already widely used in AC motor control method. So AC magnetic bearing has mature three-phase motor testing and digital control technology used for reference, thus the cost of control system of magnetic bearing can be greatly reduced. For more precise radial (two degree of freedom) control of AC magnetic bearing, building correct mathematic model of radial suspension forces is particularly important. However, the existing modeling methods for radial suspension forces of AC magnetic bearings are not enough precise [1-6]. Due to the configuration and working principle of AC magnetic bearing has similarities to the suspension subsystem of bearingless motor, thus the modeling method for radial suspension forces of bearingless motor could be reference for modeling the radial suspension forces of AC magnetic bearings. In this paper, a new radial suspension forces modeling method of AC magnetic bearing based on Maxwell tensor method is proposed, which makes modeling process more accurate compared with the conventional modeling method.

2 Configuration and Principle of AC HMB

* Contact Author Information: E-mail: zwy_729@163.com.
Address: Jiangsu University, Xuefu Road, Zhenjiang, China.
Phone Number: 13094961658.

2.1 Principle of radial suspension forces production for AC HMB

Figure 1 shows the configuration of radial AC HMB. For AC HMB, the radial suspension forces acting on the rotor consist mainly of Maxwell forces. The Maxwell forces are divided into two parts [3]: one is the forces resulting from the eccentric of rotor in bias magnetic field without control current; the other is the forces resulting from control current in bias magnetic field without the eccentric of rotor.

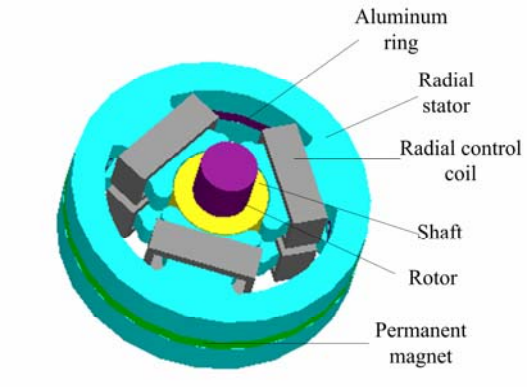

Figure 1: Configuration of Radial AC HMB

3 Mathematical Models of AC HMB

3.1 Modeling process based on Maxwell tensor method for radial suspension forces of AC HMB

3.1.1 Forces acting on the rotor

According to Maxwell tensor method, the Maxwell forces per unit area dS along dimensional angle θ on the rotor surface can be expressed as

$$dF(\theta) = \frac{B^2(\theta,t)\cdot dS}{2\mu_0} = \frac{B^2(\theta,t)}{2\mu_0}\cdot(lrd\theta) \tag{1}$$

Where l is the equivalent length of rotor, r is radius of rotor, and μ_0 is the permeability of the vacuum.

Owing to the eccentricity of the rotor caused by disturbance force f, the resulting forces per unit area dS along dimensional angle θ on the rotor surface can be expressed as

$$dF_j(\theta) = \frac{B^2(\theta,t)\cdot dS}{2\mu_0} + f\cdot dS = \frac{B^2(\theta,t)}{2\mu_0}\cdot(lrd\theta) + f\cdot dS \tag{2}$$

The equations of the Maxwell forces are broken down into components Fx and Fy in the x-axis and y-axis.

$$\begin{cases} dF_x(\theta) = dF(\theta)\cos\theta = \dfrac{B^2(\theta,t)\cdot lr\cos\theta}{2\mu_0}d\theta \\ dF_y(\theta) = dF(\theta)\cos\theta = \dfrac{B^2(\theta,t)\cdot lr\sin\theta}{2\mu_0}d\theta \end{cases} \tag{3}$$

The expression of the eccentric angle is as follows

$$\alpha = \arctan(y_0 / x_0) \tag{4}$$

The eccentric direction is defined as the direction point to the minimum air-gap length. That is the direction of the rotor eccentricity is in the same direction with the disturbance forces.

Usually the rotor eccentricity can be expressed by the eccentricity ratio

$$\varepsilon = \frac{\sqrt{{x_0}^2 + {y_0}^2}}{\delta_0} \tag{5}$$

In this paper, the Maxwell Forces acting on AC HMB shall be decided jointly by the magnetic fluxes density generated by control coils and magnet permanent. Thus the two parts of magnetic fluxes density needed to be analyzed respectively, and then be summed to get the result of magnetic fluxes density.

3.1.2 Calculation of magnetic fluxes density in air-gap generated by control coils

The fundamental component of magnetic motive force in the air-gap generated by control coils is derived by neglecting the higher axial space harmonics.

$$f_2(\theta,t) = F_2 \cos(\theta - \omega t - \varphi) \tag{6}$$

Where F_2 is the amplitude of fundamental component of magnetic motive force in the air-gap generated by control coils. ϕ is the phase angle corresponding to time t equals zero， θ is ramp mechanical angle. ω is electrical angle following the change of current.

The air-gap length at the ramp angle θ can be expressed consider the rotor eccentricity as follows

$$\delta(\theta,t) = \delta_0(1 - \varepsilon\cos(\theta - \alpha)) \tag{7}$$

$$\begin{aligned} B_2(\theta,t) &= f_2(\theta,t) \cdot \frac{\mu_0}{2\delta(\theta,t)} \\ &= F_2 \cos(\theta - \omega t - \varphi) \cdot \frac{\mu_0}{2\delta_0(1 - \varepsilon\cos(\theta - \alpha))} \end{aligned} \tag{8}$$

The pole arc angle of the magnetic bearing is 90 degrees, then we can get

$$\begin{cases} F_{2\mathrm{A}} & \theta \in (-\frac{\pi}{4}, \frac{\pi}{4}) \\ F_{2\mathrm{B}} & \theta \in (\frac{5\pi}{12}, \frac{11\pi}{12}) \\ F_{2\mathrm{C}} & \theta \in (\frac{13\pi}{12}, \frac{19\pi}{12}) \end{cases} \tag{9}$$

Where

$$F_2 = \frac{3}{2}F_{2\mathrm{A}} = \frac{3}{2}F_{2\mathrm{B}} = \frac{3}{2}F_{2\mathrm{C}} = \frac{3}{2} \cdot \frac{N_3 I}{p} \tag{10}$$

$F_{2\mathrm{A}}$、$F_{2\mathrm{B}}$、$F_{2\mathrm{C}}$ are the aptitudes of the three-phase magnetic motive forces in the air-gap generated by three-phase current A, B and C. F_2 is the fundamental amplitude of the rotating magnetic motive force generated by control coils. N3 is the single-phase effective turns. I is the aptitude of the single-phase current. p is the number of poles of rotating magnetic field. The p is 1 for the AC HMB described in the paper.

The magnetic fluxes density in air-gap generated by control coils is as follows by [3]

$$B_2 = \frac{\mu_0 \cdot F_2}{2\delta_0} \tag{11}$$

Substituting the expression of F_2 into Equation (8), and the value of ε is very small, thus the quadraticterm can be ignored in calculation.

$$B_2(\theta,t) = B_2 \cos(\theta - \omega t - \varphi)(1 + \varepsilon \cos(\theta - \alpha)) \tag{12}$$

3.1.3 Calculation of magnetic fluxes density in air-gap generated by permanent magnet

The magnetic motive force generated by permanent magnet can be get as follows

$$F_1 = H_m h_m \tag{13}$$

Where H_m is magnetic intensity at work point. H_m is the length of permanent magnet in direction of magnetization.

In the condition that the rotor deviates from the equilibrium position at a given time t, the magnetic fluxes density in air-gap generated by permanent magnet at ramp mechanical angle θ can be get as follows

$$B_1(\theta,t) = F_1 \cdot \frac{\mu_0}{2\delta(\theta,t)} = \frac{F_1 \cdot \mu_0}{2\delta_0(1 - \varepsilon \cos(\theta - \alpha))} \tag{14}$$

Then also ignores the square terms of ε, we can get

$$B_1(\theta,t) = B_1(1 + \varepsilon \cos(\theta - \alpha)) \tag{15}$$

The magnetic fluxes density in air-gap generated by the permanent magnet is as follows

$$B_1 = \frac{\mu_0}{2\delta_0} \cdot H_m \cdot h_m \tag{16}$$

3.1.4 Caculation of Maxwell forces F_x, F_y

According to the principle of field intensity superposition in the air-gap, the magnetic fluxes density generated by control coils and permanent magnet B(θ, t) can be got as

$$\begin{aligned} B(\theta,t) &= B_1(\theta,t) + B_2(\theta,t) \\ &= (1 + \varepsilon \cos(\theta - \alpha)) \cdot \left(B_1 + B_2 \cos(\theta - \omega t - \varphi)\right) \end{aligned} \tag{17}$$

Due to the magnetic motive force is landed in the air-gap nearly all of poles, thus the components F_x and F_y in the x-axis and y-axis can be got as

$$\begin{cases} F_x = \int_0^{2\pi} \dfrac{B^2(\theta,t)\cdot lr\cos\theta d\theta}{2\mu_0} \\ \quad = \int_{-\frac{\pi}{4}}^{\frac{\pi}{4}} \dfrac{B^2(\theta,t)\cdot lr\cos\theta d\theta}{2\mu_0} + \int_{\frac{5\pi}{12}}^{\frac{11\pi}{12}} \dfrac{B^2(\theta,t)\cdot lr\cos\theta d\theta}{2\mu_0} \\ \quad + \int_{\frac{13\pi}{12}}^{\frac{19\pi}{12}} \dfrac{B^2(\theta,t)\cdot lr\cos\theta d\theta}{2\mu_0} \\ F_y = \int_0^{2\pi} \dfrac{B^2(\theta,t)\cdot lr\sin\theta d\theta}{2\mu_0} \\ \quad = \int_{-\frac{\pi}{4}}^{\frac{\pi}{4}} \dfrac{B^2(\theta,t)\cdot lr\sin\theta d\theta}{2\mu_0} + \int_{\frac{5\pi}{12}}^{\frac{11\pi}{12}} \dfrac{B^2(\theta,t)\cdot lr\sin\theta d\theta}{2\mu_0} \\ \quad + \int_{\frac{13\pi}{12}}^{\frac{19\pi}{12}} \dfrac{B^2(\theta,t)\cdot lr\sin\theta d\theta}{2\mu_0} \end{cases} \tag{18}$$

Due to the values of ε and B_2 are both too small, for simplicity, we will just ignore the square terms of them and the simplified expression can be got as follows

$$\begin{cases} F_x = \dfrac{lr}{2\mu_0}\left(\dfrac{3\pi}{2}B_1B_2\cos\varphi + \dfrac{3\pi}{2}\varepsilon {B_1}^2\cos\alpha\right) \\ F_y = \dfrac{lr}{2\mu_0}\left(\dfrac{3\pi}{2}B_1B_2\sin\varphi + \dfrac{3\pi}{2}\varepsilon {B_1}^2\sin\alpha\right) \end{cases} \tag{19}$$

In Equation (19), the former is the controlled radial suspension force generated by control coils, which can adjust the distribution of magnetic field in air-gap by adjusting the control current in control coils.

E. **Calculation of Maxwell forces F_{ix}, F_{iy}**

From Equation (11), (16) and (19), and using the Clark transformation of coordinates, the controlled radial suspension force generated by control coils F_{ix} and F_{iy} can be written as

$$\begin{aligned} F_{ix} &= \frac{3\pi lrH_m h_m\mu_0\cdot\frac{3}{2}\cdot N_3 I\cos\varphi}{16{\delta_0}^2} = \frac{3\pi lrH_m h_m\mu_0 N_3\cdot(\frac{3}{2}\cdot I\cos\varphi)}{16{\delta_0}^2} \\ &= \frac{3\pi lrH_m h_m\mu_0 N_3}{16{\delta_0}^2}\cdot i_{xc} \\ F_{iy} &= \frac{3\pi lrH_m h_m\mu_0\cdot\frac{3}{2}\cdot N_3 I\sin\varphi}{16{\delta_0}^2} = \frac{3\pi lrH_m h_m\mu_0 N_3\cdot(\frac{3}{2}\cdot I\sin\varphi)}{16{\delta_0}^2} \\ &= \frac{3\pi lrH_m h_m\mu_0 N_3}{16{\delta_0}^2}\cdot i_{yc} \end{aligned} \tag{20}$$

Where i_{xc}, i_{yc} are the current components in x-axis and y-axis transformed from the synthetic current of three-phase currents by a Clark coordinate transformation.

Some conventional and practical relationships are used for the following derivation process, and the expressions are as follows

.

$$\begin{bmatrix} i_x \\ i_y \end{bmatrix} = \frac{N_3}{N_2} \begin{bmatrix} 1 & -\frac{1}{2} & -\frac{1}{2} \\ 0 & \frac{\sqrt{3}}{2} & -\frac{\sqrt{3}}{2} \end{bmatrix} \begin{bmatrix} i_A \\ i_B \\ i_C \end{bmatrix} \tag{21}$$

Where i_A、i_B，i_C are three-phase control currents. N_2 is each phase effective coil turns of equivalent two-phase coils. i_x、i_y are control currents translated by 3/2 coordinate transformation.
Where

$$\frac{N_3}{N_2} = \sqrt{\frac{2}{3}} \tag{22}$$

Thus

$$\begin{bmatrix} i_x \\ i_y \end{bmatrix} = \frac{N_3}{N_2} \cdot \begin{bmatrix} i_{xc} \\ i_{yc} \end{bmatrix} \tag{23}$$

$$\begin{bmatrix} i_{xc} \\ i_{yc} \end{bmatrix} = \frac{N_2}{N_3} \cdot \begin{bmatrix} i_x \\ i_y \end{bmatrix} \tag{24}$$

Due to the total power is identical to the original system after transformation, the expression by simple Clark coordinate transformation as Equation (20) shows can be revised by 3/2 coordinate transformation as follows

$$\begin{cases} F_{ix} = \dfrac{3\pi l r H_m h_m \mu_0 N_3}{16{\delta_0}^2} \cdot i_{xc} = \dfrac{\sqrt{3}}{\sqrt{2}} \cdot \dfrac{3\pi l r H_m h_m \mu_0 N_3}{16{\delta_0}^2} \cdot i_x \\ F_{iy} = \dfrac{3\pi l r H_m h_m \mu_0 N_3}{16{\delta_0}^2} \cdot i_{yc} = \dfrac{\sqrt{3}}{\sqrt{2}} \cdot \dfrac{3\pi l r H_m h_m \mu_0 N_3}{16{\delta_0}^2} \cdot i_y \end{cases} \tag{25}$$

3.1.5 Calculation of Maxwell forces F_{lx}, F_{ly}

In Equation (19), the later is the Maxwell force generated due to the rotor eccentricity, which is proportional to the eccentricity with the direction of the eccentric rotor. The Maxwell force components in x-axis and y-axis F_{ix} and F_{iy} of single piece of AC HMB can be written as

$$\begin{cases} F_{lx} = \dfrac{3\pi l r \varepsilon {B_1}^2}{16{\delta_0}^2} \cdot \cos\alpha = \dfrac{3\pi l r \varepsilon {H_m}^2 {h_m}^2 \mu_0}{16{\delta_0}^2} \cdot \cos\alpha \\ \quad = \dfrac{3\pi l r {H_m}^2 {h_m}^2 \mu_0}{16{\delta_0}^3} \cdot x \\ F_{ly} = \dfrac{3\pi l r \varepsilon {B_1}^2}{16{\delta_0}^2} \cdot \sin\alpha = \dfrac{3\pi l r \varepsilon {H_m}^2 {h_m}^2 \mu_0}{16{\delta_0}^2} \cdot \sin\alpha \\ \quad = \dfrac{3\pi l r {H_m}^2 {h_m}^2 \mu_0}{16{\delta_0}^3} \cdot y \end{cases} \tag{26}$$

3.1.6 Calculation of Maxwell forces F_{xx}, F_{yy}

Due the AC HMB has two pieces of stator and the calculation above are based on single piece, thus the Maxwell force acting on the rotor is virtually two times the calculation results of single piece, and the expression is as follows

$$\begin{cases} F_{xx} = 2F_{ix} + 2F_{lx} \\ \quad = \dfrac{\sqrt{3}}{\sqrt{2}} \cdot \dfrac{3\pi lrH_m h_m \mu_0 N_3}{8{\delta_0}^2} \cdot i_x + \dfrac{3\pi lrH_m{}^2 h_m{}^2 \mu_0}{8{\delta_0}^3} \cdot x \\ F_{yy} = 2F_{iy} + 2F_{ly} \\ \quad = \dfrac{\sqrt{3}}{\sqrt{2}} \cdot \dfrac{3\pi lrH_m h_m \mu_0 N_3}{8{\delta_0}^2} \cdot i_y + \dfrac{3\pi lrH_m{}^2 h_m{}^2 \mu_0}{8{\delta_0}^3} \cdot y \end{cases} \tag{27}$$

The resulting forces acting on the rotor should be sum of the radial suspension forces and the disturbance force. The equations of the Maxwell forces are broken down into components F_x and F_y in the x-axis and y-axis with a disturbance force set to f are as follows

$$\begin{cases} F_{jx} = \dfrac{\sqrt{3}}{\sqrt{2}} \cdot \dfrac{3\pi lrH_m h_m \mu_0 N_3}{8{\delta_0}^2} \cdot i_x + \dfrac{3\pi lrH_m{}^2 h_m{}^2 \mu_0}{8{\delta_0}^3} \cdot x + f_x \\ F_{jy} = \dfrac{\sqrt{3}}{\sqrt{2}} \cdot \dfrac{3\pi lrH_m h_m \mu_0 N_3}{8{\delta_0}^2} \cdot i_y + \dfrac{3\pi lrH_m{}^2 h_m{}^2 \mu_0}{8{\delta_0}^3} \cdot y + f_y \end{cases} \tag{28}$$

where F_{jx}、F_{jy} are the components of resulting force F_j in the x-axis and y-axis. f_x、f_y are the components of disturbance force f in the x-axis and y-axis.

3.2 Modeling process based on equivalent magnetic circuit method for radial suspension forces of AC HMB

In [6], a detailed derivation process of modeling process based on equivalent magnetic circuit method for radial suspension forces of AC HMB is presented. Thus the modeling process is no longer restarted here, and the expression is as follows

$$\begin{bmatrix} F_{xx} \\ F_{yy} \end{bmatrix} = \sqrt{\frac{3}{2}} K_{ir} \begin{bmatrix} 1 & 0 \\ 0 & 1 \end{bmatrix} \begin{bmatrix} i_x \\ i_y \end{bmatrix} + \frac{3}{2} K_{xy} \begin{bmatrix} 1 & 0 \\ 0 & 1 \end{bmatrix} \begin{bmatrix} x \\ y \end{bmatrix} \tag{29}$$

Where the expression of K_{ir} (force-current coefficient) is $K_{ir} = \dfrac{\mu_0 N_3 F_1 S}{2{\delta_0}^2}$, K_{xy} (force-displacement coefficient) is $K_{xy} = \dfrac{\mu_0 F_1^2 S}{2{\delta_0}^3}$, S is the equivalent area of the pole. Thus the resulting force acting on the rotor is as follows

$$\begin{bmatrix} F_{jx} \\ F_{jy} \end{bmatrix} = \begin{bmatrix} F_{xx} \\ F_{yy} \end{bmatrix} + \begin{bmatrix} f_x \\ f_y \end{bmatrix} \tag{30}$$

3.3 Contrastive result of two methods

In order to validate the feasibility of the presented method, this section will make a comparison of modeling results using two methods. The S in K_{ir} may be decided by the structure of AC HMB: the l (equivalent length of rotor) in Equation (1) is the partial rotor parameters for single piece of stator for AC HMB. The designed air-gap length is 0.5mm, while the actual work air-gap length is 0.25mm due to the limitation of assistant bearing. Thus the sum of S (equivalent area of each pole) is close to the rotor surface area in integral expression of Maxwell force. Due to the pole arc angle of the magnetic bearing is 90 degrees (1/4 circumference), thus equivalent area of each pole is close to the 1/4 rotor surface area.

$$S = \frac{1}{4} \cdot 2\pi r \cdot l \tag{31}$$

Thus K_{ir} can be expressed as

$$K_{ir} = \frac{\mu_0 N_3 F_1 S}{2\delta_0^{\,2}} = \frac{\mu_0 N_3 F_1 \pi r l}{4\delta_0^{\,2}} \tag{32}$$

Similarly, K_{xy} can be expressed as

$$K_{xy} = \frac{\mu_0 F_1^{\,2} S}{2\delta_0^{\,3}} = \frac{\mu_0 F_1^{\,2} \pi r l}{4\delta_0^{\,3}} \tag{33}$$

Substituting $F_1 = H_m h_m$ into Equation (32) and Equation (33), we can get that

$$K_{ir} = \frac{\mu_0 N_3 F_1 S}{2\delta_0^{\,2}} = \frac{\mu_0 N_3 \cdot H_m h_m \cdot \pi r l}{4\delta_0^{\,2}} \tag{34}$$

$$K_{xy} = \frac{\mu_0 F_1^{\,2} S}{2\delta_0^{\,3}} = \frac{\mu_0 F_1^{\,2} \pi r l}{4\delta_0^{\,3}} = \frac{\mu_0 \cdot H_m^{\,2} h_m^{\,2} \cdot \pi r l}{4\delta_0^{\,3}} \tag{35}$$

Thus the resulting force acting on rotor is as follows

$$\begin{aligned} \begin{bmatrix} F_{jx} \\ F_{jy} \end{bmatrix} &= \sqrt{\frac{3}{2}} \cdot \frac{\mu_0 N_3 \cdot H_m h_m \cdot \pi r l}{4\delta_0^{\,2}} \begin{bmatrix} 1 & 0 \\ 0 & 1 \end{bmatrix} \begin{bmatrix} i_x \\ i_y \end{bmatrix} \\ &+ \frac{3}{2} \cdot \frac{\mu_0 \cdot H_m^{\,2} h_m^{\,2} \cdot \pi r l}{4\delta_0^{\,3}} \begin{bmatrix} 1 & 0 \\ 0 & 1 \end{bmatrix} \begin{bmatrix} x \\ y \end{bmatrix} + \begin{bmatrix} f_x \\ f_y \end{bmatrix} \end{aligned} \tag{36}$$

Compare Equation (28) and Equation (36), the two expressions are consistent in form. For K_{xy}, the minor difference is almost solely based on multiple of the relationship between the equivalent area of each pole and rotor surface area corresponding to the region of each pole. For K_{ir}, the only difference in two expressions is a multiple of the relationship of 3/2 between them, under the condition that the equivalent area of each pole is approximated as rotor surface area corresponding to the region of each pole.

4 Experiment and Analysis

4.1 Experimental Analysis on model of radial suspension forces

The model of radial suspension forces for AC HMB built in the paper is a linearized model round the equilibrium position, thus only the applicable linear range of radial suspension has actually been tested. Due to the particularity of structure and the consistency on force/current coefficient and force/displacement coefficient in *x*-axis and *y*-axis, thus the experiment process can be simplified. So tests have been done only about the relationship of control current, eccentric displacement and radial suspension forces in one direction, which is enough to test the accuracy of the established model.

4.2 Experimental results

According to the analysis method on how to tests the relationship between the control current and radial suspension force, and the relationship between the eccentric displacement and radial suspension force, the experiment have been done and the datas have been collected and recorded. Comparison between the test result and simulation results adopting two modeling methods with MATLAB software is shown in Figure 2.

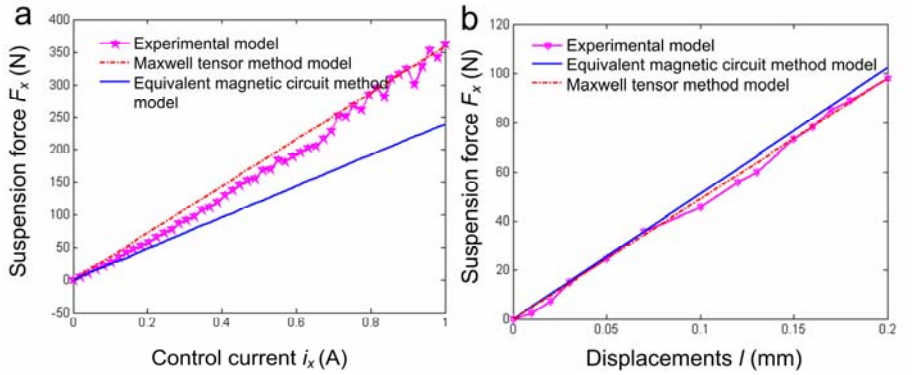

Figure 2: Comparison diagram between simulation and test results

From Figure 2, we can see that compared to with the equivalent magnetic circuit method, the results with the improved Maxwell tensor method for radial suspension forces of AC HMB are more close to the experiment result. That said, now a more accurate method has been found, which starts from the fundamental suspension principle of AC magnetic bearing to the goal that making the established model very close to the real model.

5 Conclusions

In this paper, the correctness of the model for radial suspension forces of AC HMB with the proposed method is verified by the same modeling results with the equivalent magnetic circuit method. And the experiment results show that the model based on the Maxwell tensor method is more close to the experiment results. Thus, the new modeling method based on Maxwell tensor method makes the modeling results on radial suspension forces of AC HMB more accurate compared with the equivalent magnetic circuit method, it also can be a guide for some other structure and types of AC magnetic bearing.

6 Acknowledgment

This work is sponsored by National Natural Science Foundation of China under Grant 60974053, Six Talent Flood Tide Project of Jiangsu Province under Grant 2011-ZZ026, Graduate Education Innovation Project of Jiangsu Province under Grant CXZZ12_0688 and CXZZ11_0570, and Funded by the Priority Academic Program Development of Jiangsu Higher Education Institutions.

References

[1] P. T. McMullen, C. S. Huynh, R. J. Hayes. Combination radial-axial magnetic bearing. In *4th* international symposium on magnetic bearings, August, 2000.

[2] Yan L. Xu, Yue Q. Dun, Xiu H. Wang, and Y. Kong. Analysis of hybrid magnetic bearing with a permanent magnet in the rotor by FEM. *IEEE Trans. Magn.*, 42(4), 2006.

[3] Shao R. Zhang, Ai G. Wu, Tong H. Li. Direct control for rotor eccentric displacement of bearingless permanent magnet-type synchronous motors. (in Chinese) *Proc. CSEE*, 27(12), 2007.

[4] R. Schob, C. Redemann, T. Gempp. Radial active magnetic bearing for operational with 3-phase power converter. In *4th* international symposium on magnetic bearings, August, 2000.

[5] Y. Li, W. Li, and Yong P. Lu. Computer-aided simulation analysis of a novel structure hybrid magnetic bearing. *IEEE Trans. Magn.*, 44(10), 2008.

[6] Huang Q. Zhu, Yu X. Shen, Qing H. Wu, et al. Modeling and Control System for AC Hybrid Magnetic Bearing. (in Chinese) *Proc. CSEE*, 29(18), 2009.